*Euro. Jnl of Applied Mathematics* (2011), *vol.* 22, *pp.* 317–331.  
doi:10.1017/S0956792511000076

# Steady state solutions of a bi-stable quasi-linear equation with saturating flux

M. BURNS and M. GRINFELD

*Department of Mathematics and Statistics, University of Strathclyde, Glasgow, G1 1XH, UK*
*email*: martin.f.burns@strath.ac.uk

(*Received 5 February 2010; revised 18 January 2011; accepted 19 January 2011; first published online 17 February 2011*)

In this paper, we consider the bi-stable equation proposed by Rosenau to replace the Allen–Cahn equation in the case of large gradients. We discuss the bifurcation problem for stationary solutions of this equation on an interval as the diffusion coefficient and the length of the interval are varied, concentrating on classical solutions.

**Key words:** Prescribed mean curvature equation; bi-stable non-linearity; stationary solutions

## 1 Introduction

In [13, 14], Rosenau suggested a generalisation of the Ginzburg–Landau theory to the case of large spatial gradients in the order parameter. In brief, he starts with the free energy functional

$$\mathscr{F}[u] = \int_\Omega [W(u) + \epsilon P(\nabla u)]\, dx, \tag{1.1}$$

where $\epsilon > 0$, $W(u)$ is the double-well bulk energy, e.g.

$$W(u) = \frac{u^4}{4} - \frac{u^2}{2},$$

and the interface energy $P(s)$ is a convex function of its variable that grows linearly in $s$; for example, we can take

$$P(s) = \sqrt{1+s^2} - 1.$$

Then, the $L^2$-gradient flow of (1.1) is

$$u_t = \epsilon \nabla \cdot (\psi(\nabla u)) + f(u), \tag{1.2}$$

where $f(u) = -W'(u)$,

$$\psi(s) = P'(s) = \frac{s}{\sqrt{1+s^2}},$$

and $(x,t) \in \Omega \times (0,T) \equiv Q_T$ for some bounded domain $\Omega \subset \mathbb{R}^n$, $T > 0$. Of course (1.2) has to be supplemented with some suitable boundary and initial conditions, and here, we consider the physically relevant Neumann boundary conditions (BCs), $\nabla u \cdot \underline{n}$ on $\partial\Omega$.

From now on, we work in the one-dimensional situation. Local existence and uniqueness results for weak (variational inequality) solutions to (1.2) for the particular case where

$f(u) \equiv 0$ have been established by Dascal *et al.* [3]. A well-posedness result for (1.2) with a bi-stable non-linearity $f(u)$ is proven in [2]. Weak solutions of (1.2) are defined via a variational inequality

$$\int_{Q_T} (u_t - f(u))(v-u)\,dx\,dt + \epsilon \int_{Q_T} (P(v_x) - P(u_x))\,dx\,dt \geqslant 0, \tag{1.3}$$

for all $v \in BV(Q_T)$. Note that classical solutions of (1.2) with Neumann BCs automatically satisfy variational inequality (1.3). In one space dimension, $\Omega = (0, L)$, the stationary problem for (1.2) with $\lambda = 1/\epsilon$ and the above choices for $W(u)$ and $P(u_x)$ is then

$$-\left(\frac{u'}{\sqrt{1+(u')^2}}\right)' = \lambda f(u), \quad x \in (0, L), \quad + \text{ BCs.} \tag{1.4}$$

We define a stationary BV solution of (1.2) to be a solution of the variational inequality

$$-\lambda \int_\Omega f(u)(v-u)\,dx + \int_\Omega P(v_x) - P(u_x)\,dx \geqslant 0 \ \ \forall v \in BV(\Omega), \tag{1.5}$$

obtained from (1.3) by taking $u$ to be independent of time $t$. Again, observe that in one dimension, the classical stationary solutions of (1.2) with Neumann BCs, i.e. solutions to (1.4) + $u'(0) = u'(L) = 0$, satisfy the variational inequality (1.5).

The boundary value problem (1.4) for different choices of the non-linearity $f(u)$ and BCs has received attention from a variety of authors including Pan [11], Bonheure *et al.* [1], Obersnel [10] and Habets and Omari [9]. In [9], Habets and Omari study (1.4) with Dirichlet BCs, taking $f(u) = u^p$, for $p > 0$, and they investigate the influence of the concavity of this choice of $f(u)$ on the multiplicity of solutions to the problem. Note that they can consider (1.4) only on the unit interval $[0, 1]$, as $u^p$ is homogeneous of degree $p$ and so it is possible to scale the fixed parameter $L$ out of the space domain as follows: set $y = x/L$ and $v = u/L$, and then, $v(y)$ satisfies

$$-\frac{\ddot{v}}{(1+(\dot{v})^2)^{\frac{3}{2}}} = \mu f(v), \quad x \in [0, 1],$$

where $\mu = L\lambda L^p$, and the over-dot denotes differentiation with respect to $y$. Thus, in the case of [9], it is possible to incorporate the length $L$ of the domain in the parameter $\mu$, and hence, in this case, the associated bifurcation diagram cannot change as $L$ is changed. Note that the same is also true for the semi-linear case $\psi(s) = s$ which gives the Allen–Cahn equation. Pan [11] however studied a variant of the Liouville, Bratu–Gelfand problem, taking an exponential non-linearity, $f(u) = e^u$, and both in his case and our case of $f(u) = u - u^3$, the non-linearities are non-homogeneous so that different bifurcation behaviour in $\lambda$ is in principle possible for different values of $L$. This is indeed the case as we shall demonstrate below.

In this paper, we concentrate on the analysis of classical, i.e. $C^2((0, L)) \cap C^1([0, L])$ solutions of (1.4) with the physically significant Neumann BCs
$u'(0) = u'(L) = 0$. This we do by using time maps. In the last section of the paper, we

https://doi.org/10.1017/S0956792511000076 Published online by Cambridge University Press

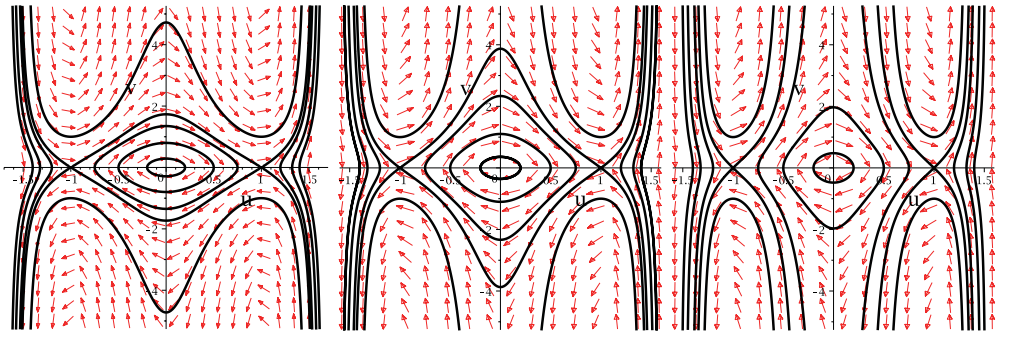

FIGURE 1. (Colour online) Phase portraits with $\lambda = 2$, $\lambda = 3$ and $\lambda = 5$.

also comment on non-classical (in fact, *discontinuous*) weak solutions of the variational inequality related to the boundary value problem (1.4).

## 2 Phase plane analysis

We rewrite (1.4) as a first-order system

$$\begin{aligned} u' &= v, \\ v' &= -\lambda(1+v^2)^{\frac{3}{2}} f(u). \end{aligned} \tag{2.1}$$

It is not hard to check that this system has

$$H(u,v) = 1 - \frac{1}{\sqrt{1+v^2}} - \lambda W(u), \tag{2.2}$$

as a first integral.

In Figure 1, we show phase portraits of (2.1) for $\lambda = 2, 3, 5$. Figure 1 indicates that there exists a value $\lambda_* \in (3,5)$ such that for all $\lambda > \lambda_*$ there are no heteroclinic solutions connecting the saddle points at $(\pm 1, 0)$. Let us consider this point in more detail.

**Proposition 2.1** *For each $\lambda \geqslant 4$, there exists a value $r_\lambda \in (0,1]$ such that:*

(1) *The orbit passing through the point $(r_\lambda, 0)$ on the positive u-axis in the phase plane satisfies $u' \to -\infty$ as $u \to 0$;*

(2) *Orbits passing through points $(r,0)$, $r_\lambda < r \leqslant 1$ are such that $u' \to -\infty$ as $u$ tends to some value $\bar{u}_\lambda(r) > 0$;*

(3) *Orbits passing through points $(r,0)$, $0 < r < r_\lambda$ are such that $|u'| < \infty$ as $u \to 0$.*

**Proof** This is a simple computation using the function $H(u,v)$ of (2.2). For the value $r_\lambda \in (0,1]$ to exist, we must have $H(r_\lambda, 0) = H(0, -\infty)$. This is equivalent to requiring that $-\lambda W(r_\lambda) = 1$ for some $r_\lambda \in (0,1]$ so that

$$r_\lambda = \sqrt{1 - \sqrt{1 - \frac{4}{\lambda}}}, \tag{2.3}$$

https://doi.org/10.1017/S0956792511000076 Published online by Cambridge University Press

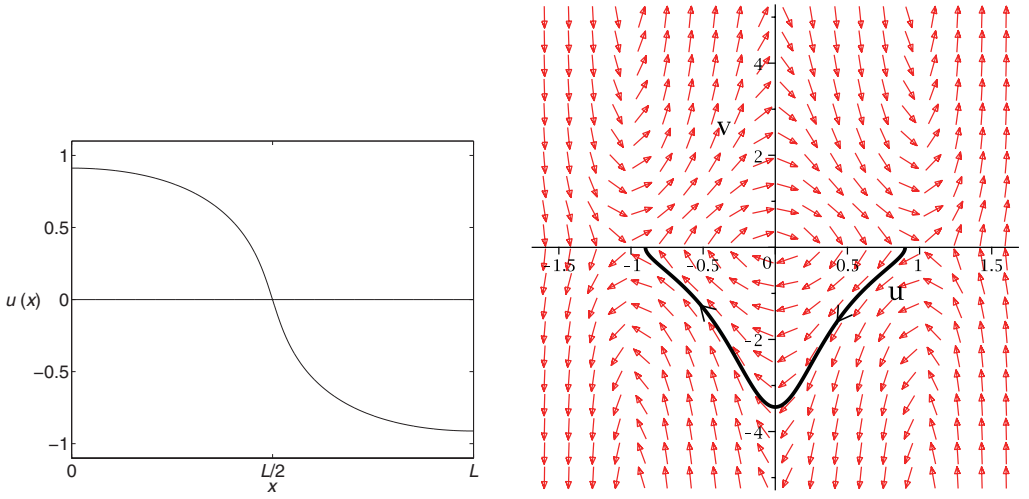


FIGURE 2. (Colour online) A classical solution to (1.4) and its corresponding phase curve.

and it is now clear that such a $r_\lambda$ would only exist for $\lambda \geqslant 4$. Note that $r_\lambda = 1$ when $\lambda = 4$ and that $r_\lambda \to 0$ as $\lambda \to \infty$.

To find the vertical asymptotes $\bar{u}_\lambda(r)$ of orbits passing through $(r, 0)$, $r \geqslant r_\lambda$ for $\lambda \geqslant 4$, we solve the equation $H(r, 0) = H(\bar{u}_\lambda(r), -\infty)$, obtaining

$$\bar{u}_\lambda(r) = \sqrt{1 - \sqrt{1 + \frac{4}{\lambda} - 2r^2 + r^4}}. \tag{2.4}$$

Of course $\bar{u}_\lambda(r_\lambda) = 0$. □

A classical solution of the Neumann problem for (1.4) is part of an orbit starting on the $u$-axis in the phase plane, which encircles the origin in a clockwise direction and ends on the $u$-axis taking a 'time' $L$ in which to do this. For example, monotone decreasing solutions start on the positive $u$-axis and end on the negative $u$-axis as shown in Figure 2. From now on we will concentrate on the multiplicity questions for monotone decreasing solutions of the Neumann problem for (1.4).

Note that for $\lambda > 4$, we can formally construct a non-classical (continuous) solution of the Neumann problem that conserves $H(u, v)$ as follows: start on the $u$-axis at $(r_\lambda, 0)$ in the phase plane and end on the negative $u$-axis at $(-r_\lambda, 0)$, and assume that $u'(L/2) = -\infty$. We will call such a solution the *critical solution* for (1.4) and we give an illustration of its form in Figure 3.

## 3 The Liapunov–Schmidt reduction

Let us define the mapping

$$\Phi : \mathbb{R} \times X \to C^0(0, L),$$

https://doi.org/10.1017/S0956792511000076 Published online by Cambridge University Press

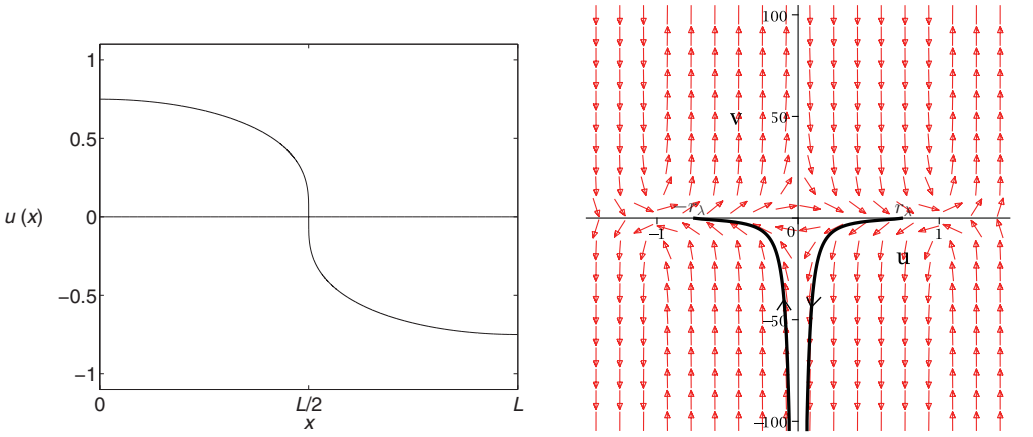


FIGURE 3. (Colour online) Critical solution of (1.4) in the Neumann case.

where $X = \{u \in C^2(0, L) : u'(0) = u'(L) = 0\}$ by

$$\Phi(\lambda, u) = \frac{u''}{(1 + (u')^2)^{\frac{3}{2}}} + \lambda f(u),$$

for $\lambda > 0$. Then, clearly the linearisation of $\Phi(\lambda, u)$ at the trivial solution $u = 0$, which we will denote by $d\Phi_{\lambda,0}$, is given by $d\Phi_{\lambda,0} \cdot v = v'' + \lambda v$.

It is obvious that the values $\lambda_k = \frac{k^2\pi^2}{L^2}$ are points of bifurcation from the trivial solution, which by the $\mathbb{Z}_2$-symmetry must be pitchforks.

We want to determine the dependence of the direction of the pitchfork on the parameter $L$. The easiest way of doing this is to use the Liapunov–Schmidt reduction [8].

$\ker(d\Phi_{\lambda,0})$ is one-dimensional when $\lambda = \lambda_k = \frac{k^2\pi^2}{L^2}$ for $k = 1, 2, \ldots$ and is spanned by $v_k = \cos\left(\frac{k\pi x}{L}\right)$. Hence, in a neighbourhood of a bifurcation point, solutions of $\Phi(\lambda, u) = 0$ on $X$ are in one-to-one correspondence with solutions of the equation $h(\lambda, y) = 0$, $y \in \mathbb{R}$ where although the bifurcation function $h$ is not known explicitly, all its partial derivatives at a bifurcation point $(\lambda_k, 0)$ can be computed by symmetry considerations and applications of the chain rule. See [8] for details. If we denote by $\langle \cdot, \cdot \rangle$ the usual inner product in $L^2$ on $[0, L]$ and set

$$d^3\Phi(v_1, v_2, v_3) = \frac{\partial^3}{\partial t_1 \partial t_2 \partial t_3} \Phi(\lambda_k, t_1 v_1 + t_2 v_2 + t_3 v_3)|_{t_1 = t_2 = t_3 = 0},$$

we have

$$h = h_y = h_{yy} = h_\lambda = 0,$$

$$h_{yyy} = \langle v_k, d^3\Phi(v_k, v_k, v_k) \rangle, \quad \text{and } h_{\lambda y} = \langle v_k, v_k \rangle$$

so that $h_{\lambda y}$ is positive for all $k$. On the other hand,

$$d^3\Phi(v_k, v_k, v_k) = -3\left(2\lambda_k v_k^3 + 3v_k''(v_k')^2\right)$$

https://doi.org/10.1017/S0956792511000076 Published online by Cambridge University Press

so that

$$h_{yyy} = 3\int_0^L \left\{ \frac{3k^4\pi^4}{L^4}\cos^2\left(\frac{k\pi\xi}{L}\right)\sin^2\left(\frac{k\pi\xi}{L}\right) - 2\frac{k^2\pi^2}{L^2}\cos^4\left(\frac{k\pi\xi}{L}\right)\right\} d\xi$$
$$= \frac{9}{8}\frac{k^2\pi^2(k^2\pi^2 - 2L^2)}{L^3}.$$

Hence, we have proved the following.

**Proposition 3.1** *The kth bifurcation from the trivial solution is a super-critical pitchfork if* $L > k\pi/\sqrt{2}$ *and a sub-critical pitchfork if the inequality is reversed.*

Note that, unlike in the semi-linear case, one can have both super- and sub-critical pitchforks for different values of $k$.

## 4 The time map

To get more information about multiplicity of solutions as we change $L$ and $\lambda$, we now define and analyse the time map for classical solutions. This is a well-known technique in the analysis of boundary value problems (see, e.g. Schaaf [15] and Smoller and Wasserman [16]). We again restrict ourselves to monotone decreasing solutions.

**Definition 4.1** We define the (classical part of the) *time map* $T_\lambda(r)$ to be the 'time' it takes for solutions starting at $u(0) = r$, $u'(0) = 0$ to reach $u = 0$.

From this definition, given that the points $(\pm 1, 0)$ are saddles, we have that the domain of the classical part of the time map, $D(T_\lambda)$, is given by

$$D(T_\lambda) = \begin{cases} (0,1) & \text{if } \lambda \leqslant 4, \\ (0, r_\lambda] & \text{if } \lambda > 4. \end{cases}$$

From the way, we have defined the classical part of the time map $T_\lambda(r)$, it is easy to see that, given $L$, for a particular value of $\lambda$, a monotone decreasing classical solution to the Neumann problem for (1.4) exists iff we can find $r \in D(T_\lambda)$ such that

$$T_\lambda(r) = \frac{L}{2},$$

(and in such case $r = u(0)$). Hence, it will be useful to compute an explicit formula for $T_\lambda(r)$ and to study its properties as we vary $\lambda$. Note that in this section, we use a mixture of analytical results and numerics.

Let $F_\lambda(u) = -\lambda W(u) = \lambda \int_0^u f(s)\,ds$. To satisfy Neumann BCs in (1.4), we must have that $H(u, u') = H(r, 0) = F_\lambda(r)$, i.e.

$$1 - \frac{1}{\sqrt{1 + (u')^2}} = F_\lambda(r) - F_\lambda(u).$$

https://doi.org/10.1017/S0956792511000076 Published online by Cambridge University Press

Solving this equality for $u'$ and setting $\chi(t) = \frac{1-t}{\sqrt{2-t}}$, as in [9], gives

$$u' = -\frac{\sqrt{F_\lambda(r) - F_\lambda(u)}}{\chi(F_\lambda(r) - F_\lambda(u))},$$

where we have taken the negative square root since we are dealing with monotone decreasing solutions. Thus, an explicit formula for $T_\lambda(r)$ is

$$T_\lambda(r) = \int_0^{T_\lambda(r)} dx = \int_0^r \frac{\chi(F_\lambda(r) - F_\lambda(u))}{\sqrt{F_\lambda(r) - F_\lambda(u)}}\, du, \tag{4.1}$$

which becomes

$$T_\lambda(r) = \int_0^r \frac{4 - 2\lambda r^2 + \lambda r^4 + 2\lambda u^2 - \lambda u^4}{\sqrt{8 - 2\lambda r^2 + \lambda r^4 + 2\lambda u^2 - \lambda u^4}\sqrt{\lambda(2r^2 - r^4 - 2u^2 + u^4)}}\, du,$$

for $f_\lambda(u) = \lambda(u - u^3)$. It is not hard to show that this is a well-defined continuously differentiable function on $D(T_\lambda)$.

Let us substitute $u = rs$ in (4.1) so that

$$T_\lambda(r) = r\int_0^1 \frac{\chi(F_\lambda(r) - F_\lambda(rs))}{\sqrt{F_\lambda(r) - F_\lambda(rs)}}\, ds := r\int_0^1 G(r,s)\, ds.$$

Computing the Taylor expansion of the function $rG(r,s)$ about the point $r = 0$ and integrating in $s$, we have

$$T_\lambda(r) = \frac{\pi}{2\sqrt{\lambda}} + \frac{3}{32}\frac{\pi(2-\lambda)}{\sqrt{\lambda}}r^2 - \frac{3}{2,048}\frac{\pi(5\lambda^2 - 20\lambda - 76)}{\sqrt{\lambda}}r^4 + O(r^6). \tag{4.2}$$

From (4.2), we can derive a number of conclusions. First of all note that for $\lambda < 2$, $T_\lambda(r)$ is initially monotone increasing, while for $\lambda > 2$, it is initially monotone decreasing. Furthermore, by (2.3), we have that $r_\lambda = O(\lambda^{-\frac{1}{2}})$ for $\lambda$ large. Therefore, since $D(T_\lambda) \to 0$ as $\lambda \to \infty$ and since the remainder term in the Taylor series (4.2) with $r = r_\lambda$ is $O(\lambda^{-\frac{1}{2}})$, we conclude that for $\lambda$ large enough, $T_\lambda(r)$ is always decreasing on $D(T_\lambda)$.

Also observe that for $\lambda \leqslant 4$, since $(u, u') = (\pm 1, 0)$ are saddle points, $\lim_{r\to 1} T_\lambda(r) = \infty$. This means that we have (at least) three different types of behaviour of the classical part of the time map, depending on the values of $\lambda$; these are indicated in Figure 4 generated using MAPLE (note the differences in vertical scale).

*Remark* We have not proved that the turning point that by the above calculation must exist for $T_\lambda(r)$ for intermediate values of $\lambda$ (as seen in Figure 4 for $\lambda = 4$) is unique and rely for that on numerical evidence.

Recall that for $\lambda > 4$, the equation

$$r = \sqrt{1 - \sqrt{1 - \frac{4}{\lambda}}}$$

gives the value of the right end-point of the domain of the classical part of the time map $T_\lambda(r)$. Solving this equation instead for $\lambda$, we obtain the inverse of $r_\lambda$ considered as a

https://doi.org/10.1017/S0956792511000076 Published online by Cambridge University Press

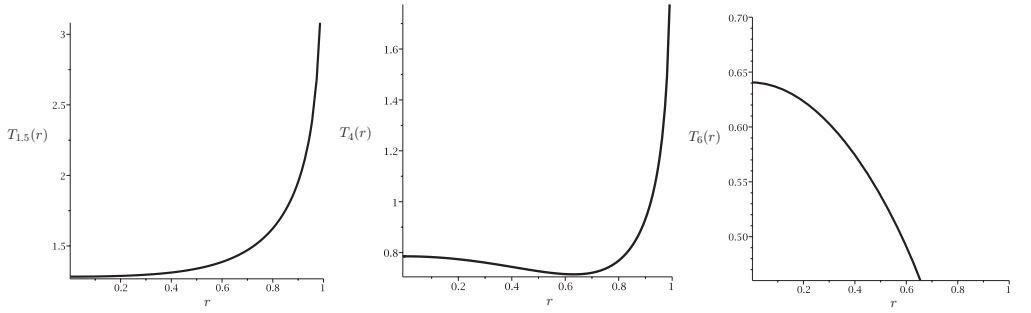


FIGURE 4. Time Maps $T_\lambda(r)$ for $\lambda = 1.5$, $\lambda = 4$ and $\lambda = 6$.

function of $r$,

$$\lambda = \Lambda(r) = \frac{4}{1-(1-r^2)^2}.$$

Hence, we can define a function

$$g(r) = T_{\Lambda(r)}(r),$$

which will give the values of the classical parts of time maps evaluated at the right end-points of their domains; this will be useful in the discussion of the bifurcation diagrams corresponding to different values of $L$. From the foregoing analysis, we see that $g(r)$ is a monotone increasing function satisfying

$$g(0) = 0, \quad \lim_{r\to 1} g(r) = \infty.$$

## 5 Bifurcation diagrams

Let us use the results obtained above to discuss the various (minimal) possibilities for bifurcation of monotone solutions to the Neumann problem for (1.4) by referring to Figures 5, 6 and 7 below. There we have plotted some of the classical parts of the time maps $T_\lambda(r)$ for values of $\lambda$ increasing down the vertical axis and we have fixed $L$ firstly to be sufficiently large, say $L_1$ (Figure 5), then intermediate, say $L_2$ (Figure 6), and finally sufficiently small, say $L_3$ (Figure 7). In the left-hand sides of these figures, we analyse how many intersections there are between $T_\lambda(r)$ (for varying values of $\lambda$) and the values of $\frac{L_i}{2}$, $i = 1, 2, 3$ and in the right-hand sides, we plot the resulting bifurcation diagrams corresponding to each value of $L_i$.

Starting with $L = L_1$ as in Figure 5. The first intersection occurs for $T_{\lambda^*}(r)$, where $\lambda_* = \pi^2/L_1^2$ and for $L_1$ sufficiently large, $\lambda_*$ will be a super-critical pitchfork bifurcation point.

There continues to be a single intersection between $T_\lambda(r)$ and $\frac{L_1}{2}$ for values of $\lambda$ up to and including $\lambda^*$ for which the intersection occurs at the value of the corresponding classical part of the time map evaluated at the right end-point of its domain (i.e. we have that $T_{\lambda^*}(r_{\lambda^*}) = \frac{L_1}{2}$). For all subsequent $\lambda$, there are no intersections between $T_\lambda(r)$ and $\frac{L_1}{2}$

https://doi.org/10.1017/S0956792511000076 Published online by Cambridge University Press

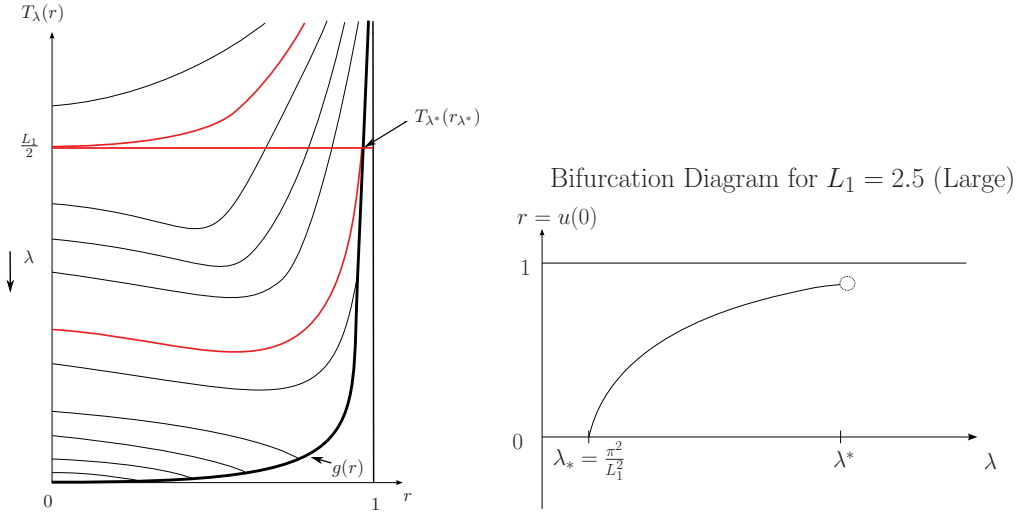


FIGURE 5. (Colour online) Plots of time maps $T_\lambda(r)$ intersecting with $\frac{L_1}{2}$ (left) and the Corresponding bifurcation diagram (right).

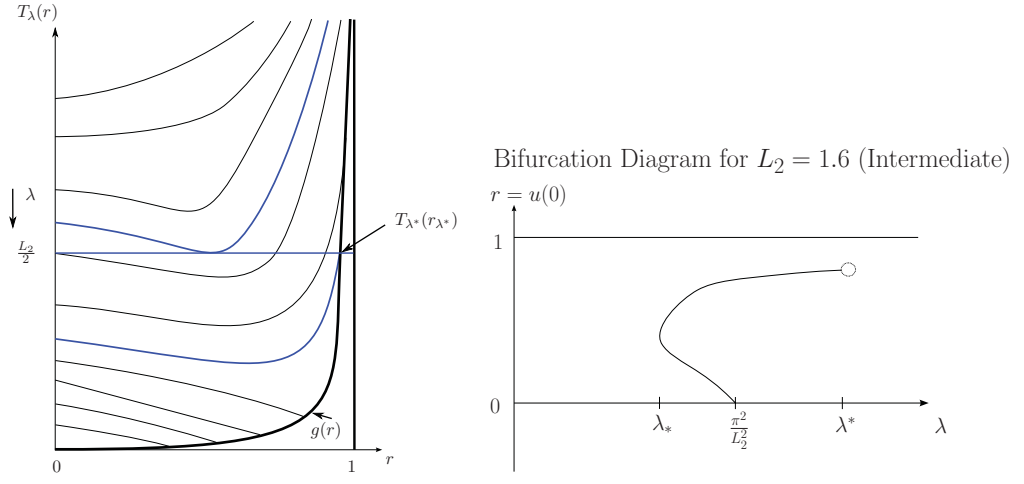


FIGURE 6. (Colour online) Plots of time maps $T_\lambda(r)$ intersecting with $\frac{L_2}{2}$ (left) and the corresponding bifurcation diagram (right).

and hence no further classical solutions to the Neumann problem. Note that the solution we obtain for the value $\lambda^*$ is the critical solution discussed in Section 2.

The intermediate values of $L$ are such that the first time map to solve the equation $T_\lambda(r) = L/2$ has a turning point. In this case, the bifurcation point is a sub-critical pitchfork and the diagram will exhibit a saddle node at some value $\lambda_*$ (see Figure 6). Again, there is a value $\lambda^*$ beyond which no classical solutions exist.

Finally, we consider $L = L_3$, the situation where the first intersection is with a monotone decreasing time map. Here, the bifurcation is again a sub-critical pitchfork, but the classical solutions stop existing before we reach a saddle node (see Figure 7).

https://doi.org/10.1017/S0956792511000076 Published online by Cambridge University Press

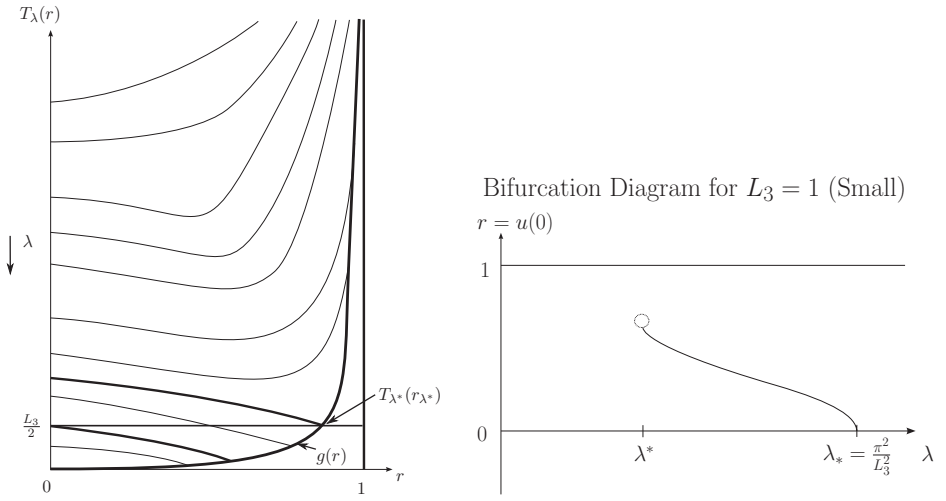


FIGURE 7. Plots of time maps $T_\lambda(r)$ intersecting with $\frac{L_3}{2}$ (left) and the corresponding bifurcation diagram (right).

## 6 Non-classical solutions to the problem

Non-classical solutions for problems related to the prescribed mean curvature equation have been considered, to some extent in [1]. However, in that paper, the non-classical solutions are $C^\infty((0, L))$. In [10], existence and multiplicity of sign-changing solutions that are possibly discontinuous at points at which the solutions attain the value zero are discussed. Below we show a construction for $\lambda > \lambda^*$ of solutions (in the BV sense) that are *discontinuous* in the interior of the interval. Moreover, we show that this construction delivers an uncountable number of solutions, and that, surprisingly, the set of solutions is dynamically stable.

For definiteness, take $L$ to be large enough so that we are discussing the super-critical case. For $\lambda > 4$, let us define a mapping $S_\lambda(r)$ as the time taken for solutions starting at $u(0) = r$, $u'(0) = 0$ (for some $r \geqslant r_\lambda$) to reach $u = \bar{u}_\lambda(r)$, where $\bar{u}_\lambda(r)$ is given by (2.4). An explicit form for $S_\lambda(r)$ is

$$S_\lambda(r) = \int_{\bar{u}_\lambda(r)}^{r} \frac{\chi(F_\lambda(r) - F_\lambda(u))}{\sqrt{F_\lambda(r) - F_\lambda(u)}}\, du,$$

where now the domain of $S_\lambda(r)$, $D(S_\lambda) = [r_\lambda, 1)$. Note that $T_\lambda(r_\lambda) = S_\lambda(r_\lambda)$.

**Definition 6.1** For a particular value of $\lambda > 4$, there exists a non-classical monotone decreasing solution to the Neumann problem if we can find $r_1, r_2 \in [r_\lambda, 1)$ (where without loss of generality, $r_1 \geqslant r_2$) such that $S_\lambda(r_1) + S_\lambda(r_2) = L$.

So for example, set $r_1 = r_2 = r^* \geqslant r_\lambda$ with $S_\lambda(r^*) = \frac{L}{2}$, we construct a (so far formal) non-classical solution to (1.4) by starting on the positive $u$-axis in the phase plane at $u = r^*$ and ending on the negative $u$-axis at $u = -r^*$ as depicted in Figure 8. There will need to be a jump connecting the two trajectories from the 'point' $(\bar{u}_\lambda(r^*), -\infty)$ to the

https://doi.org/10.1017/S0956792511000076 Published online by Cambridge University Press

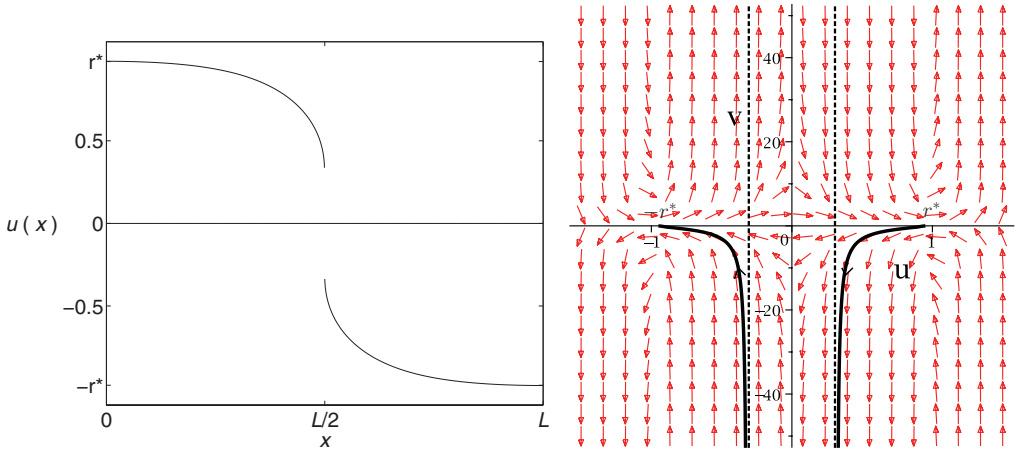


FIGURE 8. (Colour online) Non-classical solution with zero mean.

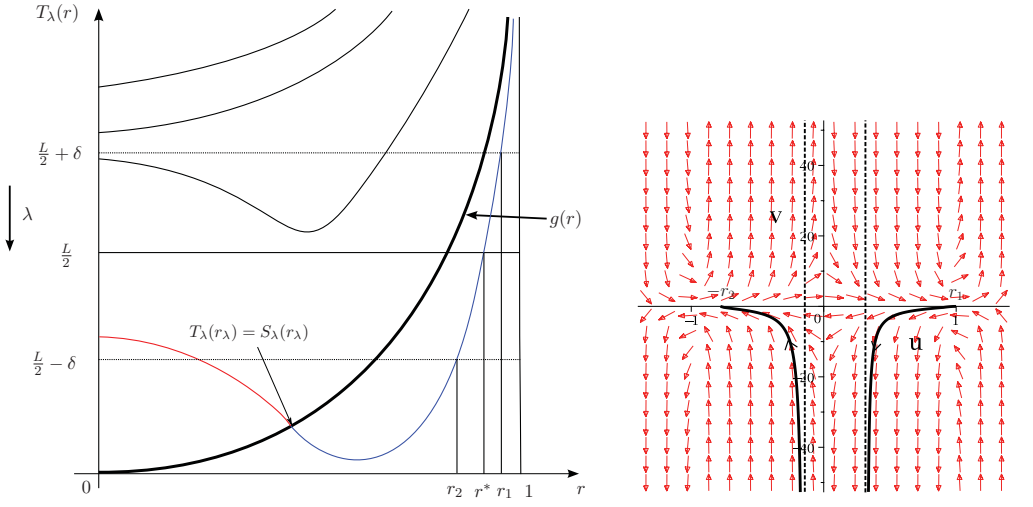


FIGURE 9. (Colour online) Construction of a non-classical solution.

'point' $(-\bar{u}_\lambda(r^*), -\infty)$ and in this way, we would have constructed a non-classical solution to (1.4) which has zero mean and obviously $S_\lambda(r^*) + S_\lambda(r^*) = L$.

We can also construct non-classical solutions to (1.4) for a particular value of $\lambda$ that do not have zero mean: we could start on the positive $u$-axis in the phase plane at $u = r_1 > r_\lambda$ and end on the negative $u$-axis at $u = -r_2 < -r_\lambda$ with $r_1 > r_2$. Again, there will have to be a jump to connect the two trajectories from the 'point' $(\bar{u}_\lambda(r_1), -\infty)$ to the 'point' $(-\bar{u}_\lambda(r_2), -\infty)$, and to satisfy the BCs, we must have $S_\lambda(r_1) + S_\lambda(r_2) = L$. Figure 9(left) gives an indication of how one can construct such a non-classical solution with positive mean: we have a value of $\frac{L}{2}$ and, for a particular value of $\lambda$, we have merged the classical (red) and non-classical (blue) time maps, $T_\lambda$ and $S_\lambda$ with an intersection between $S_\lambda(r)$ and $\frac{L}{2}$ at the value of this non-classical part of the time map evaluated at $r = r^*$, which corresponds to the non-classical solution with zero mean constructed in Figure 8. If we

https://doi.org/10.1017/S0956792511000076 Published online by Cambridge University Press

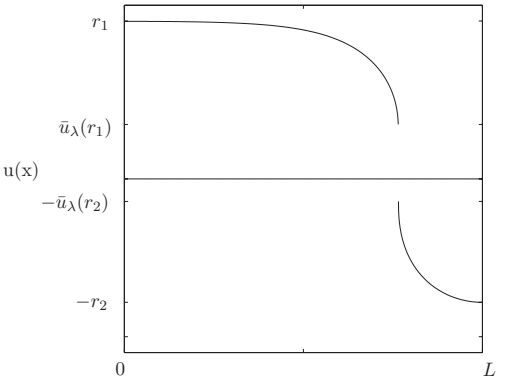


FIGURE 10. A non-classical solution of (1.4) with positive mean.

move up in the diagram from $\frac{L}{2}$ by a certain amount $\delta$ with $S_\lambda(r_1) = \frac{L}{2} + \delta$ and move down by the same amount $\delta$ with $S_\lambda(r_2) = \frac{L}{2} - \delta$ then we will indeed have constructed a non-classical stationary solution to the problem satisfying $S_\lambda(r_1) + S_\lambda(r_2) = L$ as required.

The above constructions are formal but we can show that they define BV solutions to the Neumann problem (1.4), i.e. they satisfy the variational inequality (1.5). We have the following theorem:

**Theorem 6.2** *Suppose there exists $x_0 \in (0, L)$ such that*

- *for $x \in [0, x_0)$ and for $x \in (x_0, L]$, $u(x)$ resides in level curves of the Hamiltonian $H(u, u_x)$,*
- *$S_\lambda(u(0)) + S_\lambda(u(L)) = L$, where $S_\lambda(u(0)) = x_0$ and $S_\lambda(u(L)) = L - x_0$,*
- *$u_x(x) \to -\infty$ as $x \to x_0^{\pm}$.*

*Then, $u(x)$ is a BV solution of (1.4).*

**Proof** Consider $v \in BV(\Omega)$ and the $C^\infty(\Omega)$ sequence $v_n = v * \varphi_n$ for all $n$, where $\varphi_n$ is the standard mollifier so that $v_n \to v$ with respect to the topology in $BV(\Omega)$ defined by the metric

$$d(u, v) = ||u - v||_{L^1(\Omega)} + \left| \int_\Omega |u_x| - \int_\Omega |v_x| \right|,$$

see, e.g. [6, p. 172]. Since the functional $\int_\Omega P(v_x)$ is convex, by Demengel and Temam [4, Lemma 2.2], we have that

$$\begin{aligned} &-\lambda \int_\Omega f(u)(v - u)\, dx + \int_\Omega (P(v_x) - P(u_x))\, dx \\ &\quad = \lim_{n \to \infty} \left\{ -\lambda \int_\Omega f(u)(v_n - u)\, dx + \int_\Omega (P(v_{nx}) - P(u_x))\, dx \right\}. \end{aligned}$$

https://doi.org/10.1017/S0956792511000076 Published online by Cambridge University Press

Hence,

$$
\begin{aligned}
&-\lambda\int_\Omega f(u)(v-u)\,dx+\int_\Omega (P(v_x)-P(u_x))\,dx\\
&\quad=\lim_{n\to\infty}\left\{-\lambda\int_\Omega f(u)(v_n-u)\,dx+\int_\Omega (P(v_{nx})-P(u_x))\,dx\right\}\\
&\quad=\lim_{n\to\infty}\left\{-\lambda\int_0^L f(u)(v_n-u)\,dx+\int_0^{x_0} (P(v_{nx})-P(u_x))\,dx+\int_{x_0}^L (P(v_{nx})-P(u_x))\,dx\right\}\\
&\quad\geqslant\lim_{n\to\infty}\left\{-\lambda\int_0^L f(u)(v_n-u)\,dx+\int_0^{x_0} P'(u_x)(v_{nx}-u_x)\,dx+\int_{x_0}^L P'(u_x)(v_{nx}-u_x)\,dx\right\}\\
&\quad=\lim_{n\to\infty}\left\{-\lambda\int_0^L f(u)(v_n-u)\,dx+\left[P'(u_x)(v_n-u)\right]_0^{x_0}-\int_0^{x_0}\frac{d}{dx}P'(u_x)(v_n-u)\,dx\right.\\
&\qquad\left.+\left[P'(u_x)(v_n-u)\right]_{x_0}^{L}-\int_{x_0}^{L}\frac{d}{dx}P'(u_x)(v_n-u)\,dx\right\}\\
&\quad=\lim_{n\to\infty}\left\{-\int_0^{x_0}\left[\lambda f(u)+\frac{d}{dx}\psi(u_x)\right](v_n-u)\,dx-\int_{x_0}^{L}\left[\lambda f(u)+\frac{d}{dx}\psi(u_x)\right](v_n-u)\,dx\right.\\
&\qquad\left.+\lim_{x\to x_0^-}\psi(u_x)(v_n-u)-\lim_{x\to x_0^+}\psi(u_x)(v_n-u)\right\}\\
&\quad=\lim_{n\to\infty}\left\{-\int_0^{x_0}\left[\lambda f(u)+\frac{d}{dx}\psi(u_x)\right](v_n-u)\,dx-\int_{x_0}^{L}\left[\lambda f(u)+\frac{d}{dx}\psi(u_x)\right](v_n-u)\,dx\right.\\
&\qquad\left.-v_n(x_0)+u(x_0^-)+v_n(x_0)-u(x_0^+)\right\}\\
&\quad>\lim_{n\to\infty}\left\{-\int_0^{x_0}\left[\lambda f(u)+\frac{d}{dx}\psi(u_x)\right](v_n-u)\,dx-\int_{x_0}^{L}\left[\lambda f(u)+\frac{d}{dx}\psi(u_x)\right](v_n-u)\,dx\right\}\\
&\quad=0
\end{aligned}
$$

because $u(x)$ must satisfy the Euler equation (1.4) in regions for which $u(x)$ is classical. Thus, we obtain

$$-\lambda\int_\Omega f(u)(v-u)\,dx+\int_\Omega (P(v_x)-P(u_x))\,dx\geqslant 0,\quad \forall v\in BV(\Omega).$$

□

As we show below, the set of BV solutions constructed above has dynamical stability properties: we can generate quite easily initial conditions for which the dynamic problem

$$u_t=\left(\frac{u_x}{\sqrt{1+(u_x)^2}}\right)_x+\lambda f(u),\quad x\in(0,L),$$

with Neumann BCs converges as $t\to\infty$ to a discontinuous solution such as in Figures 8 or 10 and certainly not to a spatially homogeneous solution. Taking $L=2.5$ (super-critical) with $\lambda=5$, we present the time evolution of the initial function $u_0(x)=-0.9\tanh\left[100\left(\left(\frac{x}{L}\right)-0.765\right)\right]$ in Figure 11.

https://doi.org/10.1017/S0956792511000076 Published online by Cambridge University Press

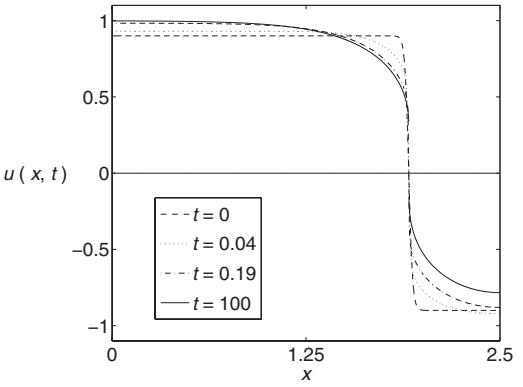


FIGURE 11. Time evolution of the initial data $u_0(x) = -0.9 \tanh\left[100\left(\left(\frac{x}{L}\right) - 0.765\right)\right]$.

In other words, it appears that the discontinuous equilibria constructed above are normally stable in $BV(\Omega)$ in the sense of [12]; we expect that the generalised principle of linearised stability developed in that work should be applicable in this situation.

## 7 Conclusions

In this paper, we started the investigation of a boundary value problem associated with a quasi-linear reaction–diffusion equation with a bi-stable kinetic non-linearity and Neumann BCs. The results are surprising.

Firstly, the bifurcation structure depends on the length of the interval, which is not the case for the corresponding semi-linear equation, for equations with diffusion governed by, say, the $p$-Laplacian operator, or indeed for equations with diffusion governed by the prescribed mean curvature operator as here, with a homogeneous kinetic non-linearity. A physical interpretation of a length-scale defined by $L$ (in addition to one defined by $\epsilon$) is required.

Secondly, as we show in Section 6, the problem possesses a wealth of apparently stable discontinuous stationary solutions, which reminds one of the situation in the integro-differential analogue of the Allen–Cahn equation [5, 7]. For comparison, the classical Allen–Cahn equation with Neumann BCs has no stable non-constant solutions, as a bifurcation analysis easily shows. Clearly, the elucidation of the mechanism by which stability is generated is an interesting open question.

## Acknowledgement

We are grateful to the anonymous referees for their helpful comments and suggestions for this paper, some of which helped to simplify the proof of Theorem 6.2.

## References


[1] Bonheure, D., Habets, P., Obersnel, F. & Omari, P. (2007) Classical and non-classical solutions of a prescribed curvature equation. *J. Differ. Equ.* **243**, 208–237.

[2] Burns, M. (2011) *Reaction-Diffusion Equations with Saturating Flux*, Ph.D. thesis. University of Strathclyde, UK.

[3] Dascal, L., Kamin, S. & Sochen, N. (2005) A variational inequality for discontinuous solutions of degenerate parabolic equations. *Rev. R. Acad. Cien. Ser. A Math.* **99**, 243–256.

[4] Demengel, F. & Temam, R. (1984) Convex functions of a measure and applications. *Indiana Univ. Math. J.* **33**, 673–709.

[5] Duncan, D. B., Grinfeld, M. & Stoleriu, I. (2000) Coarsening in an integro-differential model of phase transitions. *Eur. J. Appl. Math.* **11**, 561–572.

[6] Evans, L. C. & Gariepy R. F. (1992) *Measure Theory and Fine Properties of Functions*, CRC Press, Boca Raton.

[7] Fife, P. C. (1996) An integro-differential analog of semilinear parabolic PDEs. In: *Partial Differential Equations and Applications*, Marcel Dekker, New York.

[8] Golubitsky, M. & Schaeffer, D. G. (1985) *Singularities and Groups in Bifurcation Theory*, Springer-Verlag, New York.

[9] Habets, P. & Omari, P. (2007) Multiple positive solutions of a one-dimensional prescribed mean curvature problem. *Commun. Contemp. Math.* **9**, 701–730.

[10] Obersnel, F. (2007) Classical and non-classical sign changing solutions of a one-dimensional autonomous prescribed curvature equation. *Adv. Nonlinear Stud.* **7**, 1–13.

[11] Pan, H. (2009) One-dimensional prescribed mean curvature equation with exponential nonlinearity. *Nonlinear Anal.* **70**, 999–1010.

[12] Prüss, J., Simonett, G. & Zacher, R. (2009) On convergence of solutions to equilibria for quasilinear parabolic problems. *J. Differ. Equ.* **246**, 3902–3931.

[13] Rosenau, P. (1989) Extension of Landau-Ginzburg free-energy functionals to high-gradient domains. *Phys. Rev. A* **39**, 6614–6617.

[14] Rosenau, P. (1990) Free-energy functionals at the high-gradient limit. *Phys. Rev. A* **41**, 2227–2230.

[15] Schaaf, R. (1991) *Global Solution Branches of Two Point Boundary Value Problems*, Springer-Verlag, Berlin.

[16] Smoller, J. & Wasserman, A. (1981) Global bifurcation of steady state solutions. *J. Differ. Equ.* **39**, 269–290.